Characteristic Changes of the S_2/S_1 Difference FTIR Spectrum Induced by Ca^{2+} Depletion and Metal Cation Substitution in the Photosynthetic Oxygen-Evolving Complex†

Yukihiro Kimura,* Koji Hasegawa, and Taka-aki Ono*

Laboratory for Photo-Biology, RIKEN Photodynamics Research Center, The Institute of Physical and Chemical Research, 519-1399 Aoba, Aramaki, Aoba, Sendai 980-0845, Japan

Received December 26, 2001; Revised Manuscript Received March 13, 2002

ABSTRACT: Effects of Ca^{2+} depletion and substitution with other metal cations on the structure of the protein matrices of the oxygen-evolving complex (OEC) and their corresponding changes upon the S_1 to S_2 transition were examined using Fourier transform infrared (FTIR) spectroscopy. Ca^{2+} depletion and further supplementation with Li^+, Na^+, Mg^{2+}, Ca^{2+}, or Sr^{2+} did not significantly affect the typical vibrational features in the double difference S_2/S_1 spectrum, including the symmetric [1365(+)/1404(−) cm^{-1}] and the asymmetric [1587(+)/1566(−) cm^{-1}] stretching modes of the carboxylate ligand and the amide I and II modes of the backbone polypeptides. On the other hand, supplementation with K^+, Rb^+, Cs^+, or Ba^{2+} significantly modified the S_2/S_1 spectrum, in which the carboxylate modes disappeared and the amide I and II modes were modified. Results indicate that the binding of metal cations that have ionic radii larger than that of Ca^{2+} to the Ca^{2+} site induces perturbations in the protein matrices in the vicinity of the Mn cluster to interrupt the characteristic structural and/or conformational changes upon the oxidation of the Mn cluster accompanied with the S_1 to S_2 transition. The spectrum was also altered by the supplementation of Cd^{2+}, which has an ionic radius comparable to that of Ca^{2+}. A single-pulse-induced S_2/S_1 difference spectrum revealed that bands that have been assigned to the vibrational modes for the Y_Z tyrosine and the histidine ligand for the Mn cluster were not induced in the K^+-supplemented membranes, although the histidine band is likely to be preserved in the Ca^{2+}-depleted membranes. The Y_Z band was considerably small in the double difference S_2/S_1 spectrum in the Ca^{2+}-depleted and the cation-substituted membranes but distinctively present in the Sr^{2+}- or Ca^{2+}-replenished membranes. Furthermore, cation supplementation induced several new bands that disappeared following the Ca^{2+} replenishment. These results suggest that the proper organization of the hydrogen bond network within OEC for the water oxidation chemistry requires the Ca^{2+} ion and indicate that the role of Ca^{2+} is not purely structurally defined by the physical properties of the ion, such as valence and ionic radius. On the basis of these and other findings, we propose that Ca^{2+} is necessary for the formation of the hydrogen bond network that is involved in the reaction step of water oxidation.

Photosynthetic oxygen evolution is catalyzed by the oxygen-evolving complex (OEC),[1] which is comprised of a tetranuclear Mn cluster, a redox-active tyrosine Y_Z (tyrosine 161 of the D1 protein), one Ca^{2+} ion, and one or several Cl^- ion(s). Water oxidation occurs through five intermediate states, labeled as S_n ($n = 0-4$), where S_0 is the lowest reduced state. The OEC cumulatively accumulates oxidizing equivalent by successive absorption of four photons at the PS II reaction center and attains the highest oxidation state (S_4) after accumulating four oxidizing equivalents. Subsequently, the S_4 state is reduced back to the S_0 state concomitant with the release of an oxygen molecule (reviewed in refs *1*−*4*).

Depletion of one Ca^{2+} ion per OEC results in the loss of the O_2-evolving capability, which is restored by replenishment with Ca^{2+} or, to a lesser extent, with Sr^{2+} (*5*−*10*). In the absence of Ca^{2+}, the OEC can be oxidized to the S_2 state, but further oxidation steps beyond the S_2 state are interrupted (*11*−*15*). Therefore, the Ca^{2+} ion is considered as an indispensable inorganic cofactor for O_2 evolution. A set of EXAFS studies on Sr^{2+}-substituted PS II membranes showed the location of Sr^{2+} at a distance of 3.4−3.5 Å from the Mn cluster (*16*, *17*). Spectroscopic studies using ^{113}Cd NMR on ^{113}Cd-substituted PS II membranes indicated that one Cd^{2+}-bound site per PS II exists in the vicinity of the Mn cluster, which affects the ^{113}Cd NMR through its electron spin (*18*).

† This work was supported by grants for the Frontier Research System at RIKEN and Grant-in-Aid for Scientific Research (13640659) (to T.O.) from MECSST of Japan.

* To whom correspondence should be addressed. Telephone: +81 (22) 228 2047. Fax: +81 (22) 228 2045. E-mail: ykimura@postman.riken.go.jp; takaaki@postman.riken.go.jp.

[1] Abbreviations: OEC, oxygen-evolving complex; PS, photosystem; Chl, chlorophyll; DCMU, 3-(3, 4-dichlorophenyl)-1,1-dimethylurea; MES, 2-morpholinoethanesulfonic acid; Bis-Tris, bis-(2-hydroxyethyl)-iminotris(hydroxymethyl)methane; Q_A, primary quinone acceptor of photosystem II; Q_B, secondary quinone acceptor of photosystem II; Y_Z, redox-active tyrosine 161 of the D1 protein; EXAFS, extended X-ray absorption fine structure; EPR, electron paramagnetic resonance; NMR, nuclear magnetic resonance; TL, thermoluminescence; FTIR, Fourier transform infrared; EDTA, ethylenediamine-*N*,*N*,*N*′,*N*′-tetraacetic acid.

10.1021/bi016093u CCC: $22.00
Published on Web 04/16/2002

These results imply the presence of the Ca^{2+} in a close proximity to the Mn cluster. In contrast, a separate EXAFS study has detected a small change at 2.7 Å Mn−Mn distance, but changes were not detected in the Fourier peak at 3.3 Å when Ca^{2+} was replaced with Sr^{2+} or Dy^{3+} (*19*). EPR experiments on the Mn^{2+}-supplemented PS II membranes indicated that the Mn^{2+} ion that occupies the Ca^{2+}-site is located outside the first coordination sphere of the Mn cluster (*20*). Site-directed mutagenesis studies using the cyanobacterium *Synechocystis* 6803 have demonstrated that mutants at Asp-59 and Asp-61 in the A−B loop of the D1 protein require higher Ca^{2+} concentrations in the culture medium for photoautotrophic growth, suggesting that these residues are involved in the Ca^{2+} binding (*21*, *22*). Recently, the X-ray crystallographic structure, at 3.8 Å resolution of the PS II core from *Synechococcus elongatus*, indicated that the Mn cluster is located on the lumenal side of the D1 protein; unfortunately, the study did not provide any detailed information on the location of the Ca^{2+} ion (*23*).

It has been reported that the Ca^{2+} site of OEC can be occupied by other metal cations (*9*−*11*, *24*−*30*). Studies probing the effects due to the cation substitutions on the properties of OEC may provide a clue to the elucidation of the role of Ca^{2+} in the photosynthetic water oxidation. The order of the relative affinities of the cations to a Ca^{2+} site is as follows: trivalent cations > divalent cations > monovalent cations. This order has been accounted by the properties of the Ca^{2+} site, which resides in the coordination sphere with polynegative charges (*30*). Kinetic analyses suggested that a lanthanide cation can be bound to the Ca^{2+} site with a very high affinity and is difficult to replace it by Ca^{2+} due to extremely slow off-rate from the site (*24*, *27*, *28*, *30*). Depending on the substituted lanthanide species, the lanthanide-substituted OECs exhibited various modified S_2 states, in terms of their redox properties, as revealed by the $S_2Q_A^-$ TL band with varied peak temperatures (*28*); however, S_2 EPR signals were not detected (*24*, *27*). It has been indicated that a divalent metal cation can be bound to the Ca^{2+} site in a competitive manner and that Sr^{2+} can functionally substitute for Ca^{2+} (*5*, *9*−*11*, *26*, *30*). EPR studies for the Sr^{2+}-substituted OEC revealed that the magnetic property of the Mn cluster was altered, as indicated by the formation of a modified S_2 multiline signal and the enhancement of the $g = 4.1$ signal (*7*, *11*, *12*). The normal S_2 state formation was suggested for the Mg^{2+}-substituted OEC but not for the Ba^{2+}-substituted OEC (*13*). An important divalent cation for probing the Ca^{2+} site is Cd^{2+}, which has an ionic radius very similar to that of Ca^{2+} (*31*). The Cd^{2+}-substituted OEC showed neither the $g = 4.1$ nor the multiline signals, although the TL band due to the $S_2Q_A^-$ charge recombination was normal compared with that induced in the O_2-evolving control OEC (*11*). ^{113}Cd NMR spectroscopy demonstrated the proximity of the Mn cluster to the ^{113}Cd-bound Ca^{2+}-site, in which $^{113}Cd^{2+}$ is located in a symmetrical six-coordinate sphere of oxygen and nitrogen or chlorine (*18*). Monovalent alkali metal cations were also used as tools for probing the Ca^{2+} site (*9*, *25*, *26*, *29*, *30*), since they have the same electronic configuration as that of their alkali earth metal congeners but less one positive charge. Affinities of the alkali metal cations to the Ca^{2+} site depended on their ionic radii; cations with ionic radii larger than that of Ca^{2+} (K^+, Rb^+, and Cs^+) showed interactions with the Ca^{2+} site; however, cations with smaller ionic radii (Li^+ and Na^+) showed much lower affinity to the site (*29*). The redox and magnetic properties of the S_2 state OEC were significantly modified when the Ca^{2+} site was occupied by K^+, Rb^+, or Cs^+, as revealed by the disappearance of the S_2 state EPR signals and by the formation of a TL band with elevated peak temperatures (*29*).

Most of the previously utilized experimental techniques for studying the effects of Ca^{2+} depletion and the cation substitution on the properties of OEC, however, cannot elucidate possible changes in the protein matrices of OEC that provide crucial information for understanding the function of Ca^{2+} in OEC. In recent years, FTIR difference spectroscopy has been extensively applied for studying S state dependent changes in microenvironments of protein matrices of OEC, including the ligands of the Mn cluster as well as water molecules interacting with OEC (*32*−*50*). It was reported that the vibrational modes found in the S_2/S_1 difference FTIR spectrum were inhibited in Ca^{2+}-depleted PS II membranes, suggesting that Ca^{2+} is directly responsible for the light-induced structural changes of the carboxylate ligand for the Mn cluster (*33*). However, we have demonstrated that the Ca^{2+} ion is not required for structural changes of the putative carboxylate ligand (*50*). An FTIR study in the low-frequency region showed that the Sr^{2+} substitution caused a small structural perturbation that affected the bond strength of the Mn−O−Mn cluster in the PS II OEC (*43*). In the present paper, we studied the effects of Ca^{2+} depletion and the substitution with monovalent (alkali metal) and divalent (alkali earth metal and Cd^{2+}) cations on the S_2/S_1 difference FTIR spectrum. On the basis of the results and other findings, the structural as well as functional roles of Ca^{2+} in the photosynthetic oxygen evolution are discussed.

MATERIALS AND METHODS

Sample Materials. BBY-type O_2-evolving PS II membranes (*51*) were prepared from spinach with modifications (*52*) and stored in liquid N_2 until use. The PS II membranes were suspended in a medium containing 2 M NaCl, 400 mM sucrose, and 20 mM Mes/NaOH, pH 6.5 (medium A), at 0.5 mg of Chl/mL. The suspension was gently stirred at 0 °C for 25 min under weak light for the depletion of the functional Ca^{2+} as well as the 24 and 16 kDa extrinsic proteins. The following procedures were performed under complete darkness or dim green light unless otherwise noted. The membrane suspension was further incubated at 0 °C for 10 min after adding 0.06 g of neutralized Chelex 100 (100−200 mesh)/1 mg of chlorophyll and washed once with medium A in the presence of Chelex 100. Then, the membranes were washed twice with a medium containing 400 mM sucrose (Sigma Ultra) and 20 mM Bis-Tris-HCl (medium B) at pH 6.5 in the presence of Chelex 100. The resulting Ca^{2+}-depleted membranes, suspended in Chelex-treated medium B, were further incubated at 0 °C in complete darkness for over 3 h and stored in liquid N_2 until use. In some cases, Chelex was omitted from medium A, which did not affect the properties of the resulting Ca^{2+}-depleted membranes. OEC was relaxed to the S_1 state during the incubation, as revealed by the absence of the S_2 multiline signal. All wares used in the experiments for Ca^{2+} depletion were rinsed with acid.

Sample Preparations for Measurements. Sample membranes were suspended in Chelex-treated medium B at 0.5 mg of Chl/mL supplemented with the indicated metal cations and then incubated at 0 °C for 5 min in darkness. Detectable changes were not observed in the FTIR spectra and TL bands by extending the incubation time up to 12 h. Sample suspensions included 0.1 mM DCMU (50 mM dimethyl sulfoxide solution as stock) for measuring the light-induced $S_2Q_A^-/S_1Q_A$ difference spectrum or 0.1 mM DCMU and 10 mM NH_2OH for the light-induced Q_A^-/Q_A difference spectrum. NH_2OH and DCMU were added as an adventitious electron donor and as an inhibitor of the electron transfer from Q_A to Q_B, respectively. For single-pulse-induced S_2/S_1 difference spectra, the sample membranes were suspended in Chelex-treated medium B at pH 6.0 unless otherwise noted. The membranes were incubated at 0 °C for 5 min in darkness in the presence of the indicated cations, followed by the addition of 2 mM potassium ferricyanide and 18 mM potassium ferrocyanide as the electron acceptor and redox buffer for keeping the non-heme iron on the acceptor side of PS II in a reduced state (*35*). Both ferricyanide and ferrocyanide were added as sodium salts when indicated. The membranes were precipitated by centrifugation for 30 min at 176000*g*, and the resulting pellet was sandwiched between a pair of ZnSe or BaF_2 disks. Sample manipulations for FTIR were performed under complete darkness using a NightVision binocular (Kokusen D-2MV I) equipped with the appropriate short-wavelength cutoff filter. Metal cations were added as their chlorides with a grade of 99.9% purity, except for RbCl (99.8% purity).

Measurements. FTIR spectra were recorded on a vacuum-type spectrophotometer (Bruker IFS-66v/s) equipped with an MCT detector (EG&G Optoelectronics J15D16-M204B-S01M-60-D316/6) (*50*). A custom-made CdTe band-pass filter (2000−350 cm^{-1}) was placed in front of the sample membranes to block the He−Ne laser beam leaking from the interferometer compartment and to improve the signal-to-noise ratio. The sample temperature was maintained at 250 K using a homemade cryostat and a temperature controller (Chino, KP1000). Samples were illuminated with either CW light (Hoya-Schott HL150R) passing through a long-path filter (≥620 nm) for the Q_A^-/Q_A difference and $S_2Q_A^-/S_1Q_A$ difference spectra or a single flash provided from a nanosecond Nd^{3+}:YAG laser (Spectra Physics INDI-50, 532 nm, pulse width 6−7 ns) for the single-pulse-induced S_2/S_1 difference spectrum. The difference spectra were obtained by subtracting the dark spectra from those following illumination. Each single-beam spectrum with 150 scans (65 s accumulation) was measured at 4 cm^{-1}. Five to seven difference spectra were averaged to improve the signal-to-noise ratio. The double difference S_2/S_1 spectrum was obtained by subtracting the Q_A^-/Q_A difference spectrum from the $S_2Q_A^-/S_1Q_A$ difference spectrum. Thermoluminescence was measured using a homemade apparatus. Membrane samples suspended in Chelex-treated medium B (pH 6.5) at 0.25 mg of Chl/mL were incubated at 0 °C for 5 min in the dark after addition of the indicated divalent cations. DCMU (50 μM) was added to the suspension to ensure a single turnover from the S_1 to the S_2 state. The suspensions were illuminated at 250 K with CW light (>630 nm) for 5 s followed by rapid cooling in liquid N_2, and the resulting light emission during sample warming was recorded against sample temperature (*52*).

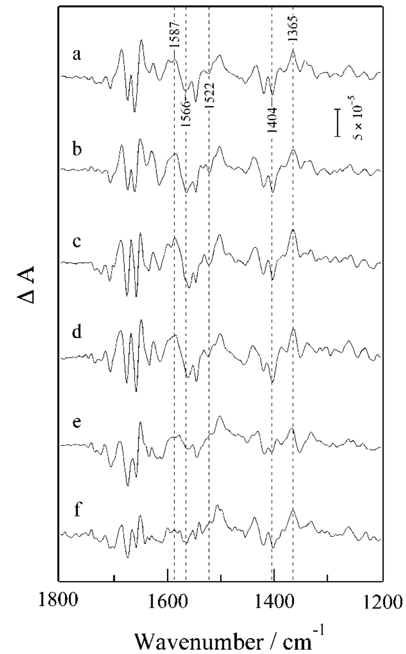

FIGURE 1: Double difference S_2/S_1 spectra of Ca^{2+}-depleted PS II membranes with (a) no addition, (b) $MgCl_2$, (c) $CaCl_2$, (d) $SrCl_2$, (e) $BaCl_2$, and (f) $CdCl_2$. Sample membranes in Bis-Tris-HCl buffer (pH 6.5) were supplemented with 20 mM divalent cations and were incubated at 0 °C for 5 min under darkness. Each S_2/S_1 spectrum was obtained by subtracting the light-induced Q_A^-/Q_A difference spectrum from the light-induced $S_2Q_A^-/S_1Q_A$ difference spectrum (see text for details). Samples membranes were illuminated with continuous light (2 mW/cm^2) at 250 K for 10 s. The sample suspension included 0.1 mM DCMU for the $S_2Q_A^-/S_1Q_A$ difference spectrum or 0.1 mM DCMU and 10 mM NH_2OH for the Q_A^-/Q_A difference spectrum.

RESULTS

Effects of Divalent Cations. An S_2/S_1 difference FTIR spectrum can be conventionally obtained by subtracting a dark spectrum from a light spectrum induced by a single flash excitation. However, this method cannot be applied to the present study, except for special cases, since large amounts of K^+ (78 mM) from the redox buffer (2 mM potassium ferricyanide and 18 mM potassium ferrocyanide) must be included in the sample suspension (*35*). Instead, we have obtained the double difference S_2/S_1 spectrum by subtracting a Q_A^-/Q_A difference spectrum from an $S_2Q_A^-/S_1Q_A$ difference spectrum, after normalizing both spectra to the intensities of their CO stretching bands of Q_A^- at 1478 cm^{-1}. Although the double subtraction method provides for the measurement of S_2/S_1 difference spectra under various cation conditions, it may also result in the lowering of spectrum quality to some extent. Figure 1 shows the double difference S_2/S_1 spectra of the Ca^{2+}-depleted PS II membranes supplemented with 20 mM alkali earth metal cations (Mg^{2+}, Ca^{2+}, Sr^{2+}, Ba^{2+}) or Cd^{2+}. The S_2/S_1 difference spectrum of the Ca^{2+}-depleted PS II membranes (spectrum a) exhibited characteristic S_2/S_1 vibrational features, including the symmetric [1365(+)/1404(−) cm^{-1}] and asymmetric [1587(+)/1566(−) cm^{-1}] carboxylate stretching modes and the pronounced differential bands in the amide I (1700−1600 cm^{-1}) and amide II (1600−1500 cm^{-1}) regions. These

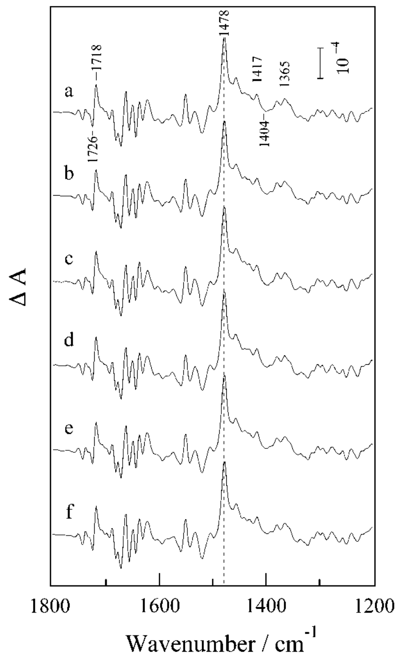

FIGURE 2: Light-induced Q_A^-/Q_A difference spectra of Ca^{2+}-depleted PS II membranes with (a) no addition, (b) $MgCl_2$, (c) $CaCl_2$, (d) $SrCl_2$, (e) $BaCl_2$, and (f) $CdCl_2$. Sample membranes in Bis-Tris-HCl buffer (pH 6.5) were supplemented with 20 mM divalent cations and were incubated at 0 °C for 5 min under darkness. Samples membranes were illuminated with continuous light (2 mW/cm^2) at 250 K for 10 s. The sample suspension included 0.1 mM DCMU and 10 mM NH_2OH. The intensity of each spectrum was normalized with respect to the Q_A^- band at 1478 cm^{-1}.

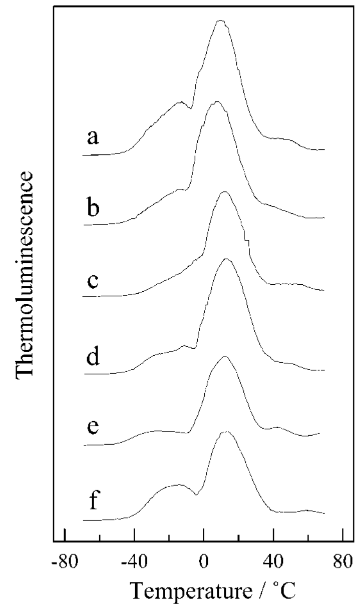

FIGURE 3: Thermoluminescence glow curves of the Ca^{2+}-depleted PS II membranes with (a) no addition, (b) $MgCl_2$, (c) $CaCl_2$, (d) $SrCl_2$, (e) $BaCl_2$, and (f) $CdCl_2$. Membrane samples in Bis-Tris-HCl buffer (pH 6.5) (250 μg of Chl/mL) were supplemented with the indicated cations and illuminated with continuous light at 250 K for 5 s in the presence of 50 μM DCMU. The small shoulder at approximately 0 °C is an artifact due to the influence of melting ice on the heating rate.

results are in agreement with those using the Mes/NaOH buffer system reported previously (*50*), in which 40 mM Na^+ was included in the sample suspension. Although these characteristic S_2/S_1 vibrational features were consistently observed for the membranes supplemented with Mg^{2+} (spectrum b), Ca^{2+} (spectrum c), or Sr^{2+} (spectrum d), the amide I bands in the Ca^{2+}-depleted and Mg^{2+}-supplemented membranes seem to be comparatively less prominent than those in the presence of Ca^{2+} and Sr^{2+}. Furthermore, close inspection of the spectra revealed small but distinct differences among the spectra, as will be discussed later. The appearance of the carboxylate modes for the Sr^{2+}-supplemented membranes at the same positions as those for the Ca^{2+}-replenished membranes indicates that the putative carboxylate does not serve Ca^{2+} with ligand and supports a previous report, which concludes that Ca^{2+} is not directly involved in the structural changes of the putative carboxylate ligand for the Mn cluster upon the S_1 to S_2 transition (*50*). However, supplementation of Ba^{2+} markedly affected the typical vibrational modes, as shown in spectrum e, with suppressed carboxylate bands and weakened amide bands. It is important to note that the intensity of the positive band at 1365 cm^{-1}, for the symmetric carboxylate mode in the double difference spectrum, may include some uncertainties because the Q_A^-/Q_A difference spectrum has a positive band at the same wavenumber (see Figure 2), whereas the intensity of the negative band at 1404 cm^{-1} is comparatively more reliable due to the absence of Q_A^-/Q_A mode at this position. Since Cd^{2+} has the same valence as Ca^{2+} and an ionic radius (0.97 Å) equivalent to that of Ca^{2+} (0.99 Å), the use of Cd^{2+} as a probe has allowed studies on the Ca^{2+}-binding site for several metalloproteins including OEC (*31*). For the Cd^{2+}-supplemented membranes (spectrum f), although the symmetric carboxylate mode at 1365(+)/1404(−) cm^{-1} appeared with relatively normal features, the asymmetric carboxylate mode at 1587(+)/1566(−) cm^{-1} was largely diminished. Additionally, the amide I and II modes were largely suppressed as compared with those of other divalent cation supplemented spectra.

Figure 2 shows the Q_A^-/Q_A difference spectra of the Ca^{2+}-depleted membranes supplemented with various divalent cations. All membrane samples revealed quite similar spectra, with bands that are characteristic of Q_A at 1718(+)/1726(−), 1478(+), 1417(+), and 1365(+) cm^{-1} as well as in the amide I and II regions. The intensities and band positions of these bands were practically identical for every spectrum, which was normalized with respect to the intensity of the Q_A^- semiquinone band at 1478(+) cm^{-1}. These results indicate that the structure and the function of the Q_A site are not influenced whatsoever by Ca^{2+} -depletion and the subsequent supplementation of divalent cations and that the acceptor side of PS II does not contribute to the observed changes of the double difference S_2/S_1 spectra.

Figure 3 shows the TL glow curves of the Ca^{2+}-depleted PS II membranes supplemented with various divalent cations. The sample membranes were illuminated in the presence of DCMU, which ensures a single turnover of PS II. TL bands appeared in a similar fashion around 10 °C for the Ca^{2+}-depleted membranes with (a) no addition or addition of 20 mM (b) Mg^{2+}, (c) Ca^{2+}, (d) Sr^{2+}, (e) Ba^{2+}, and (f) Cd^{2+} and can be assigned to the band from $S_2Q_A^-$ recombination. A sharp dip around 0 °C is an artifact due to the influence of melting ice on the heating rate. Since the microenvironment surrounding the Q_A site that was probed by FTIR is defined as normal in the Ca^{2+}-depleted and divalent cations supple-

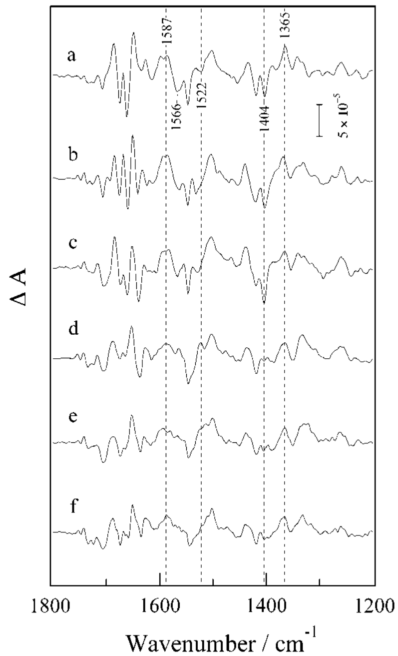

FIGURE 4: Double difference S_2/S_1 spectra of Ca^{2+}-depleted PS II membranes with (a) no addition, (b) LiCl, (c) NaCl, (d) KCl, (e) RbCl, and (f) CsCl. Sample membranes in Bis-Tris-HCl buffer (pH 6.5) were supplemented with 200 mM alkali metal cations and were incubated at 0 °C for 5 min under darkness. Each S_2/S_1 difference spectrum was obtained by subtracting the light-induced Q_A^-/Q_A difference spectrum from the light-induced $S_2Q_A^-/S_1Q_A$ difference spectrum (see text for details). The sample suspension included 0.1 mM DCMU for the $S_2Q_A^-/S_1Q_A$ difference spectrum or 0.1 mM DCMU and 10 mM NH_2OH for the Q_A^-/Q_A difference spectrum.

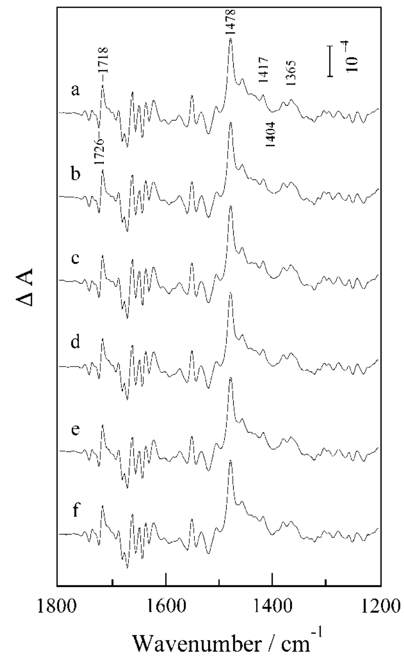

FIGURE 5: Light-induced Q_A^-/Q_A difference spectra of Ca^{2+}-depleted PS II membranes with (a) no addition, (b) LiCl, (c) NaCl, (d) KCl, (e) RbCl, and (f) CsCl. Sample membranes in Bis-Tris-HCl buffer (pH 6.5) were supplemented with 200 mM alkali metal cations and were incubated at 0 °C for 5 min under darkness. Sample membranes were illuminated with continuous light (2 mW/cm^2) at 250 K for 10 s. The sample suspension included 0.1 mM DCMU and 10 mM NH_2OH. The intensity of each spectrum was normalized with respect to the Q_A^- band at 1478 cm^{-1}.

mented membranes, as shown in Figure 2, the formation of a normal $S_2Q_A^-$ band indicates that Ca^{2+} depletion and the cation supplementation do not affect the redox potential of the S_2 state Mn cluster, despite the apparent perturbations in the S_2/S_1 vibrational features for the Ba^{2+}- and Cd^{2+}-supplemented membranes. Previously, we reported that Ba^{2+} substitution induced a TL band with elevated peak temperature (*13*), in which we used a Ca^{2+}-depleted membrane sample that was similar but not identical to that used in the present study. In the previous study, membrane preparation and TL measurements were performed in the presence of EDTA. However, the presence of EDTA cannot account for the apparent differences because the addition of EDTA was not shown to influence the TL band in the presence of Ba^{2+} (data not shown). At present, we conclude that the normal $S_2Q_A^-$ band is induced by the substitution with Ba^{2+} under the present experimental conditions, although the reason for the difference remains to be resolved.

Effects of Monovalent Cations. Figure 4 shows the double difference S_2/S_1 spectra of the Ca^{2+}-depleted PS II membranes supplemented with 200 mM alkali metal cations (Li^+, Na^+, K^+, Rb^+, or Cs^+). Although monovalent cations exhibited a much lower affinity to the Ca^{2+} site, as compared with divalent cations (*9*, *10*, *29*, *30*), monovalent cations at this concentration can sufficiently affect the redox and magnetic properties of the Mn cluster (*29*). When the Ca^{2+}-depleted membranes (spectrum a) were subjected to Li^+ (spectrum b) and Na^+ (spectrum c), the carboxylate modes appeared normal, and although their intensities were different between the two sample membranes, the amide I and amide II bands appeared at nearly the same positions as those in the Ca^{2+}-depleted OEC. On the other hand, the characteristic S_2/S_1 vibrational features were significantly modified by the supplementation of K^+ (spectrum d), Rb^+ (spectrum e), or Cs^+ (spectrum f). Both the symmetric and asymmetric carboxylate stretching bands disappeared concomitant with considerable weakening of the bands in the amide I and II regions. We note that the positive band at 1365(+) cm^{-1} was relatively prominent in the K^+-, Rb^+-, and Cs^+-supplemented membranes, and although the position of this band coincides with the symmetric carboxylate mode in the S_2 state, this band was not assigned to the carboxylate mode since other carboxylate bands [1587(+), 1566(−), and 1404(−) cm^{-1}] concurrently disappeared in these supplemented membranes. Therefore, this band may be attributable to the incomplete subtraction of the Q_A^-/Q_A spectrum, as described in detail, and/or a band other than the carboxylate. Previously, we have reported on the absence of the carboxylate modes and the modification of the amide modes in the S_2/S_1 difference FTIR spectra of Ca^{2+}-depleted membranes that were prepared by the low-pH method, in which S_2/S_1 spectrum was measured using a redox buffer (including potassium ferricyanide and potassium ferrocyanide) and in the presence of EDTA (*33*). Since the carboxylate modes and the amide modes are inhibited by K^+ ions as shown in this study, and by EDTA as previously reported (*50*), the presence of EDTA and K^+ in the sample suspension must be responsible for the absence and modifications of these vibrational modes in the previous FTIR study.

Figure 5 shows the effects of the supplementation of monovalent cations on the Q_A^-/Q_A difference spectra. It is clearly evident that the spectra of the cation-supplemented membrane samples eventually develop into spectra that are identical to that of Ca^{2+}-depleted membranes, which is identical to that of Ca^{2+}-replenished oxygen-evolving membranes (Figure 2, spectrum c). These observations indicate that the presence of relatively high concentrations of monovalent cations does not influence the Q_A and its surrounding protein environment, and therefore the significant changes in the spectral features found in the membranes supplemented with K^+, Rb^+, or Cs^+ are not attributable to modifications on the acceptor side of PS II.

The double subtraction procedure for calculating the double difference S_2/S_1 spectra may introduce constraints that reduce the quality of the spectrum and therefore limit the interpretation of the spectrum to relatively pronounced bands. Comparatively, a light-minus-dark difference spectrum that is induced by a single turnover flash can provide a more reliable S_2/S_1 spectrum. However, to eliminate light-induced redox changes of the non-heme iron on the acceptor side of PS II and accepting an electron (*35*), salts of ferricyanide/ferrocyanide must be included in the sample suspension during the measurements. This can be accomplished by obtaining the spectra of the K^+-supplemented membranes simply with the use of a redox buffer containing $K_3[Fe(CN)_6]/K_4[Fe(CN)_6]$. We also measured the single-pulse spectrum of the membranes with no further supplementation of cations and in the presence of 2 mM $Na_3[Fe(CN)_6]$/9 mM $Na_4[Fe(CN)_6]$ couple, which can prevent a large part of the redox change of the non-heme iron. Since the concentrations of the Na^+ ions in these measurements were as low as 42 mM, levels at which Na^+ may not associate to the Ca^{2+} site, the obtained spectrum will virtually correspond to the single-pulse-induced S_2/S_1 difference spectrum of the Ca^{2+}-depleted membranes without any cation substitution; however, we cannot completely exclude the possibility that the spectrum may include some modification induced by Na^+ at these low concentrations. In addition, since the affinity of the Ca^{2+} site for Na^+ is considerably lower than for Ca^{2+} (*29*, *30*), it was possible to measure the single-pulse-induced Ca^{2+}-replenished spectrum free of possible interference effects by K^+ by using the $Na_3[Fe(CN)_6]/Na_4[Fe(CN)_6]$ couple in the presence of Ca^{2+} ions. Oxygen evolution that is supported by 1 mM Ca^{2+} is only slightly affected by the presence of Na^+ ions, at least up to 150 mM (*29*).

Figure 6 shows the single-pulse-induced S_2/S_1 difference spectra of the Ca^{2+}-depleted PS II membranes at pH 6.0 supplemented with 20 mM Ca^{2+} and 78 mM Na^+ (spectrum a), 42 mM Na^+ (spectrum b), and 200 mM K^+ (spectrum c). The spectral features of the Ca^{2+}/Na^+-supplemented membranes (spectrum a) coincide well with those of the double difference spectrum of the Ca^{2+}-replenished membranes (shown in Figure 1). The Na^+(42 mM) supplemented spectrum (spectrum b) was very similar to the double difference spectra of the Ca^{2+}-depleted as well as Na^+-supplemented membranes (shown in Figure 4). Eventually, identical single-pulse spectra were observed when the concentration of Na^+ ions was increased up to 200 mM (unpublished data). Similarly, the single-pulse spectrum of the K^+-supplemented membranes (spectrum c) was comparable to the corresponding double difference spectrum (shown in Figure 4). Both the symmetric [1365(+)/1404(−) cm^{-1}] and asymmetric [1587(+)/1566(−) cm^{-1}] carboxylate stretching bands were absent concomitant with substantial modifications in the amide regions. However, some differences between the double difference and the single-pulse spectra of the K^+-supplemented membranes were evident in the 1430−1350 cm^{-1} region. In the single-pulse spectrum, three positive bands (1429, 1396, and 1373 cm^{-1}) and three negative bands (1414, 1387, and 1356 cm^{-1}) were observed; however, in the double difference spectrum, these bands were replaced by a broad and unresolved positive band at 1365 cm^{-1}. Therefore, the positive band at 1365 cm^{-1} exhibited in the double difference spectrum of the membranes supplemented with K^+, Rb^+, or Cs^+ (shown in Figure 4) may include some ambiguity. The single-pulse spectra of the K^+-supplemented membranes show broad positive bands at 1331 and 1259 cm^{-1} and a negative band at 1227 cm^{-1}. These bands were less pronounced for the Na^+(42 mM) supplemented membranes and absent or insignificant for the Ca^{2+}-

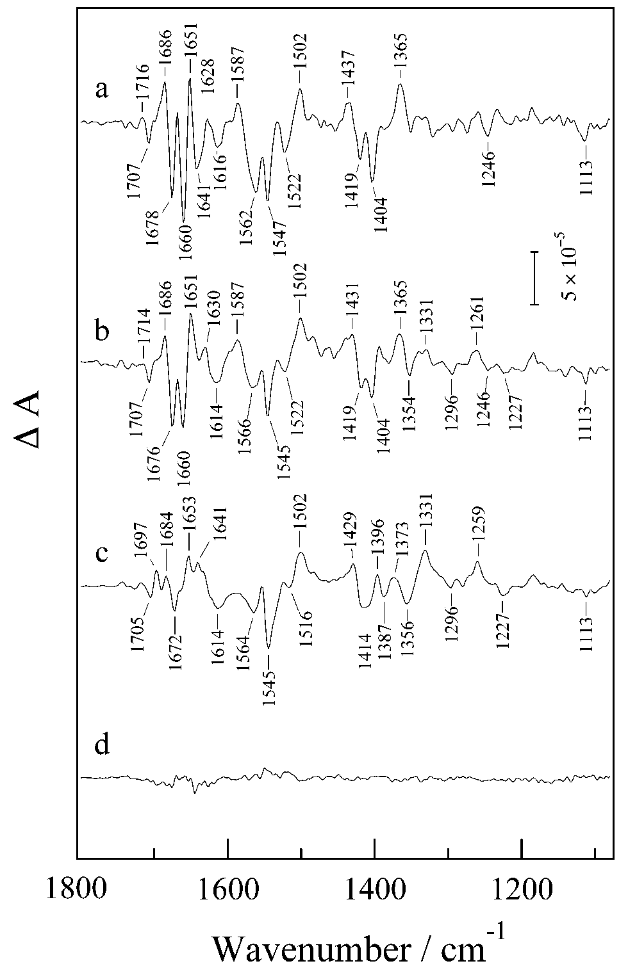

FIGURE 6: Single-pulse induced S_2/S_1 difference spectra of the Ca^{2+}-depleted PS II membranes supplemented with (a) 20 mM Ca^{2+} and 78 mM Na^+, (b) 42 mM Na^+, and (c) 200 mM K^+ in Bis-Tris-HCl buffer (pH 6.0). Sample membranes were illuminated with a single pulse from a frequency-doubled Nd^{3+}:YAG laser (6−7 ns, 532 nm, 20 mJ/cm^2) at 250 K. The sample suspension included ferricyanide (2 mM)/ferrocyanide (18 mM) for spectra a and c or ferricyanide (2 mM)/ferrocyanide (9 mM) for spectrum b as the redox couple. Supplementation was as sodium salts for spectra a and b or as potassium salts for spectrum c. Cation concentrations were adjusted by the addition of chloride salts of respective cations, if necessary. Each difference spectrum was normalized with respect to the band intensity of the ferrocyanide CN stretching mode at 2037 cm^{-1}. A dark-minus-dark FTIR spectrum (spectrum d) was presented to show a noise level.

Table 1: Effects of Metal Cation Substitution on the Properties of the Ca^{2+}-Depleted OEC

added cations	ionic radius (Å)	FTIR carboxylate band at 1404 cm^{-1}	peak temp of TL band (°C)	S_2 multiline EPR signal	O_2 evolution
none		yes	10	normal[a]	no
alkali metal					
Li^+	0.60	yes	2[a]	normal[a]	no
Na^+	0.95	yes	10[a]	normal[a]	no
K^+	1.33	no	38[a]	no	no
Rb^+	1.48	no	38[a]	no	no
Cs^+	1.69	no	38[a]	no	no
alkali earth metal					
Mg^{2+}	0.65	yes	8		no
Ca^{2+}	0.99	yes	11	normal[a]	yes
Sr^{2+}	1.13	yes	12	modified[b]	yes
Ba^{2+}	1.35	no	13		no
Cd^{2+}	0.97	yes	12	no[b]	no

[a] Ono et al. (*29*). [b] Ono and Inoue (*11*).

replenished membranes. These bands, or a portion of these bands, seem evident in the double difference spectra of the Li^+-, Na^+-, K^+-, Rb^+-, Cs^+-, or Ba^{2+}-supplemented membranes, although the existence of the bands was equivocal in the other membrane samples. Furthermore, it is important to note that the single-pulse spectrum of the Ca^{2+}-replenished membranes showed relatively small but distinct negative bands at 1522, 1246, and 1113 cm^{-1}, although the latter two bands were not resolved in the corresponding double difference spectrum (shown in Figure 1). Interestingly, these bands were largely diminished in the spectrum of the K^+-supplemented membranes. The band at 1522 cm^{-1} disappeared completely, and a very small negative band remained at 1516 cm^{-1}. The bands at 1522 and 1246 cm^{-1} were also suppressed in the Na^+(42 mM) supplemented spectrum, but the band at 1113 cm^{-1} appeared relatively prominent.

DISCUSSION

Our FTIR studies showed that the characteristic S_2/S_1 vibrational features for the Ca^{2+}-depleted membranes are modified differently by the supplementation of monovalent and divalent cations. Results indicated that the occupation of the Ca^{2+} site by a foreign cation leads to alterations of the protein matrices that participate in the Mn cluster functionally and/or structurally and thus affects their conformational and/or structural changes upon its oxidation to the S_2 state. Effects of cations on the properties of OEC, obtained from our present and previous studies (*11*, *29*), are summarized in Table 1, which includes the ionic radius of each cation. The alkali metal cations show clear correlation between their ionic radii and their effects on the properties of OEC. For K^+, Rb^+, and Cs^+, with ionic radii larger than that of Ca^{2+}, the carboxylate modes in their FTIR spectra were largely suppressed concomitant with significant alterations in the amide modes. Notably, these cations have also altered the redox and magnetic properties of the S_2 state Mn cluster, as revealed by the upshift of the TL bands and by the absence of the multiline EPR signal (*29*). On the other hand, these properties were scarcely affected by Li^+ and Na^+, with ionic radii smaller than that of Ca^{2+}. Therefore, association of Li^+ or Na^+ to the Ca^{2+} site induces insignificant perturbation in OEC, or perhaps at the concentration studied, these cations may not associate directly with the Ca^{2+} site due to their low affinities to the site.

For the alkali earth metal group, the effects of the cations on the properties of OEC seem to correlate with their ionic radii; however, the correlation is uncertain since the group contains Ca^{2+} and Sr^{2+}, which play a function in the O_2 activity. Every S_2/S_1 FTIR band, including the carboxylate mode, was retained with Mg^{2+}, a cation with an ionic radius smaller than that of Ca^{2+}; however, the bands were largely diminished and/or modified with Ba^{2+}, a cation with a larger ionic radius than that of Ca^{2+}. These results suggest that, when the Ca^{2+} site is occupied by cations with ionic radii larger than that of Ca^{2+}, structural perturbations of the protein moiety are induced, which are responsible for the disappearance and distortion of the vibrational features of the S_2/S_1 spectrum. Apparently, those perturbations may also influence the magnetic structure of the S_2 state Mn cluster in abolishing its EPR multiline signal, which would be caused by the changes in magnetic interaction and/or valence distribution among four Mn ions. For the Cd^{2+}-substituted OEC, which has been reported to not exhibit S_2 multiline signal (*11*), the FTIR spectrum was considerably and uniquely modified, in which the symmetric carboxylate bands were preserved, but the asymmetric bands disappeared, concomitant with the suppression of the amide I and II bands. Comparatively, the Cd^{2+} ion is similar to the Ca^{2+} ion with respect to their ionic radii, as well as their valences. However, the two cations are considerably different in terms of their hard−soft natures; Ca^{2+} prefers relatively hard whereas Cd^{2+} prefers relatively soft ligands (*31*, *53*). Therefore, as compared to the Ca^{2+} as well as the other alkali metal and alkali earth metal cations, the Cd^{2+} ion may associate with the Ca^{2+} site with a different configuration to induce unique modifications. It has been reported that the asymmetric carboxylate mode was selectively upshifted in D_2O, which presumably disturbs the hydrogen bonding via a water molecule between the Mn cluster and the carboxylate ligand (*34*). Using this information, a possible explanation for the effect of Cd^{2+} may be that a similarly upshifted asymmetric mode, due to perturbed hydrogen bonding, overlaps with the amide bands to be obscure.

It is important to note that Ba^{2+} and Cd^{2+} substitutions did not affect the oxidation potential of the Mn cluster, as depicted by the formation of the normal $S_2Q_A^-$ TL band, whereas K^+, Rb^+, and Cs^+ substitutions resulted in considerable decrease in the oxidation potential of the S_2 state Mn cluster (29). This suggests that the magnetic properties of the Mn cluster are more susceptible to structural alteration of the cluster rather than its redox properties. It can be presumed that monovalent cation induced perturbations are greater than those of divalent cations because monovalent cations cannot sufficiently neutralize the negative charges that probably exist in the Ca^{2+} site in OEC (*30*). Ba^{2+} has been reported to inhibit the Ca^{2+}-dependent O_2 evolution in a noncompetitive manner (*30*), suggesting that Ba^{2+} may associate to OEC at yet another site in addition to the Ca^{2+} site. Furthermore, it has been also reported that the distances between a manganese ion and its ligands were uniquely changed by Ba^{2+}, as compared to Na^+, K^+, and Ca^{2+}, in a synthetic model complex for the OEC Mn cluster with a binuclear manganese core and a binding site for a metal cation at approximately 4 Å from the core (*54*). Therefore, these unique properties of the Ba^{2+} ion may, at least in part, ascribe to the properties for the Ba^{2+}-substituted OEC.

Although the properties of the Mn cluster in the Ca^{2+}-depleted OEC, as listed in Table 1, are comparable to those of the untreated control and the Ca^{2+}-replenished OEC, Ca^{2+} depletion resulted in the loss of O_2 evolution capability. Therefore, it can be considered that the primary role of the Ca^{2+} ion in the mechanism of water oxidation is not simply structural, which stabilizes the cluster structure by associating the cluster and/or controls the redox property of the Mn cluster by optimizing the ligand environment. Furthermore, most of the prominent vibrational modes found in the S_2/S_1 spectrum may not directly be related to the Ca^{2+} functions since it was shown that Ca^{2+} depletion does not interrupt their appearances. However, the marked structural disturbances of OEC induced by the occupation of the Ca^{2+} site by cations with ionic radii larger than that of Ca^{2+} suggest that the Ca^{2+} site is located at the spot, the changes of which could influence the structure of OEC despite no marked alterations in the OEC properties in the absence of Ca^{2+}. Therefore, a good possibility is that Ca^{2+} contributes some structural change(s) of OEC upon S state transition(s) other than S_1 to S_2. This view is compatible with the finding that the features of the FTIR spectrum including the carboxylate modes showed characteristic period four behavior during the S state cycling (*46*, *47*).

As shown in Figure 6, the negative bands at 1522, 1246, and 1113 cm^{-1}, which are evident on the single-pulse-induced Ca^{2+}-replenished spectrum, were largely suppressed in the K^+-substituted spectrum. The negative band at 1522 cm^{-1} in the S_2/S_1 spectrum was assigned to the CC stretching mode of the phenol ring of the Y_Z tyrosine (*37*). The band at 1113 cm^{-1} was assigned to the CN stretching mode of the imidazole ring of the histidine residue, which is a direct ligand in the Mn cluster (*42*). In *Synechocystis* 6803, the CO stretching mode of the phenol ring of the Y_Z tyrosine is also prominent as the negative band at 1254 cm^{-1} in the S_2/S_1 spectrum, in addition to the CC stretching mode at 1522 cm^{-1} (*37*), but the band at 1254 cm^{-1} was not observed in the spectrum of PS II preparations from spinach, in which the band may possibly be overlapped by other bands in the same region. Therefore, it is not presently clear whether the band at 1246 cm^{-1} involves Y_Z or another unidentified mode. The appearances of the Y_Z and histidine modes in the S_2/S_1 spectrum indicate that the Mn cluster is connected to the histidine residue and the Y_Z tyrosine through direct coordination and through hydrogen bonds, respectively. Therefore, the suppression of these modes in the K^+-substituted spectrum implies that either the bonds are lost or the oxidation of the Mn cluster induces insignificant structural and/or conformational changes in the protein moiety including the putative bonds. By taking into account the significant distortions of the FTIR spectrum and the loss of the multiline signal by K^+ substitution (and also by Rb^+ and Cs^+ substitutions), it can be assumed that the bindings of these cations to the Ca^{2+} site lead to the liberation of the histidine ligand from the Mn cluster in OEC or the change in the valence distribution among the four Mn ions in the S_2 state cluster and thus modify the magnetic and redox properties of the Mn cluster.

Interestingly, suppression of the Y_Z band at 1522 cm^{-1} was observable in the double difference S_2/S_1 spectra of the Ca^{2+}-depleted membranes. Similarly, the band was absent or considerably suppressed in the membranes supplemented with cations, except for Ca^{2+} and Sr^{2+}, as shown in Figures 1 and 4. In the spectrum supplemented with Li^+, Na^+, or Mg^{2+}, the suppression of the 1522 cm^{-1} band is not quite obvious at one glance due to the appearance of a negative band in the same region. These results indicate that Ca^{2+} depletion results in the perturbation or destruction of the hydrogen bonding between the Mn cluster and the Y_Z tyrosine. In our studies thus far, the putative hydrogen bonding was restored by Ca^{2+} and Sr^{2+} but not by the other cations. However, we cannot completely exclude the possibility that some artifact derived by the calculation of the double difference S_2/S_1 spectrum partially contributes the features of the bands that appeared in this region.

The bands at 1246 and 1113 cm^{-1} were not resolved in the double difference spectrum, even in the Ca^{2+}-replenished membranes, and therefore the presence of these two bands in the Ca^{2+}-depleted and the cation-substituted membranes from the double difference spectra was not elucidated. However, we can estimate whether these bands are present in the Ca^{2+}-depleted spectrum by the following considerations: the OEC of the Na^+-supplemented membranes showed properties similar to those of the Ca^{2+}-depleted membranes, as shown in Table 1. Furthermore, the double difference S_2/S_1 spectrum of the Na^+-supplemented membranes was particularly similar to that of the Ca^{2+}-depleted membranes. These similarities between the Ca^{2+}-depleted and Na^+-supplemented OECs imply that possible perturbations induced by the Na^+ binding are too minor to change the basic properties of the Ca^{2+}-depleted OEC. Alternatively, at 200 mM, Na^+ may not actually be bound to the Ca^{2+} site, in consideration of the extremely low affinity of the Ca^{2+} site for Na^+ (*29*, *30*). As shown in Figure 6, the band at 1246 cm^{-1} is absent, while the band at 1113 cm^{-1} was apparently evident in the spectrum supplemented with low Na^+ concentration (42 mM). It can be assumed that the Ca^{2+} site is not occupied by Na^+ at this concentration. Therefore, the results indicate that the putative histidine band is retained in the Ca^{2+}-depleted spectrum, which is compatible with the view that the histidine band originates from the direct histidine ligand of the Mn cluster, since the normal magnetic and redox properties of the Ca^{2+}-depleted OEC suggest the normal ligation structure of the Mn cluster. It is of note in this context that the tyrosine band at 1522 cm^{-1} was largely suppressed in the spectrum, inconsistent with the result from the double difference spectrum of the Ca^{2+}-depleted membranes. A residual band intensity at 1522 cm^{-1} may be ascribed to the Ca^{2+}-preserved OEC present in the Ca^{2+}-depleted membranes (15−20%) and/or another band overlapping in this region.

A possible interpretation of the disappearance of the Y_Z band is that a hydrogen bond network around the Mn cluster and Y_Z tyrosine of OEC is distorted or partially lost by Ca^{2+} depletion. It has been proposed that this hydrogen bond network plays an essential role in the mechanism of water oxidation, in which Y_Z participates directly by abstracting protons or hydrogen atoms from substrate water which is bound to the Mn cluster (*55*−*57*). If we speculate on the basis of this scenario, the function of Ca^{2+} in OEC is involvement in the formation of the hydrogen bond network required for the water oxidation. As no other cations, with the exception of Sr^{2+}, can substitute Ca^{2+} in restoring such a network, the Ca^{2+} function is more than simply a structural cofactor in the network. It has been proposed that Ca^{2+} can act as a Lewis acid for binding a water substrate and adjusts the reactivity of the water molecule by altering its pK_a (*30*). A water molecule or a molecule derived from water which is bound to Ca^{2+} may also be involved in the network formation. For the Ca^{2+}-depleted OEC, the S state transition beyond the S_2 state is interrupted, and thus further illumination induces a split EPR signal at $g = 2$. It has been proposed that this EPR signal originates either from the Y_Z radical magnetically coupled to the Mn cluster in the S_2 state (*55*, *58*−*60*) or from the magnetic interaction between the Y_Z radical and another organic radical species (*61*, *62*). In either case, the Y_Z radical thus formed is abnormally stable and does not result in the oxidation of the S_2 state Mn cluster. It has been hypothesized that the S_2 state in the Ca^{2+}-depleted OEC is proton deficient, as compared to the normal S_2 state, and that the Y_Z radical formed in the Ca^{2+}-depleted S_2 state is hardly rereduced by the Mn cluster due to the unavailability of a proton that is required for the reduction of the neutral Y_Z radical (*63*). If this is the case, we might assume that the proton for the reduction of the neutral Y_Z radical in the S_2 state is served by the Ca^{2+}-dependent hydrogen bond network, as described herein. The split-type EPR signal was induced in the membranes depleted of Cl^-, which is another inorganic cofactor for O_2 evolution (*64*, *65*). Therefore, this may imply that the Cl^- ion is also involved in the formation of the putative hydrogen bond network.

For some cation-substituted spectra, new bands were prominent at 1331(+), 1259(+), and 1227(−) cm^{-1}. Although the origin(s) of these bands are unknown at the present, we noted that the bands are surprisingly similar to the modes of a bicarbonate that associates to the non-heme iron on the acceptor side of PS II (*36*, *49*). The bicarbonate modes at 1257(+) and 1338(+) cm^{-1} were assigned to the COH bending and the CO stretching vibrations in the reduced Fe^{2+} state, respectively, and the mode at 1228(−) cm^{-1} was ascribed to the CO stretching vibration in the oxidized Fe^{3+} state. Although one may attribute these bands to the redox change of the non-heme iron on the acceptor side of PS II, we argue against this view for the following reasons: first, the acceptor side bicarbonate modes are accompanied by a differential band at 1111(+)/1102(−) cm^{-1} and a negative band at 1094(−) cm^{-1}, which are assigned to the side chain mode of the histidine ligand for the non-heme iron (*35*, *36*). Apparently, as shown in Figure 6, such histidine modes were absent in the single-pulse-induced S_2/S_1 spectra of the K^+-substituted membranes that show prominent bands at 1331(+), 1259(+), and 1227(−) cm^{-1}, in which the redox couple of ferricyanide/ferrocyanide prevents the non-heme iron from being oxidized. Second, the bands were still evident in the double difference S_2/S_1 spectra, in which the acceptor side modes disappear from the spectrum by subtracting the Q_A^-/Q_A spectrum from the $S_2Q_A^-/S_1Q_A$ spectrum. These strongly indicate that some changes on the donor side are responsible for these modes. We should note in this context that a bicarbonate has been proposed to be involved in the events of the water oxidation and associate to the Mn cluster (*66*, *67*). Therefore, although these modes were not observed in the spectrum of the oxygen-evolving PS II, the modes may arise from the bicarbonate that is bound to the Mn cluster.

In conclusion, the present results indicate that the redox and magnetic properties of the Mn cluster in the cation-substituted OEC depend on the ionic radius and valence of the foreign cation in the Ca^{2+}-binding site. Ca^{2+} depletion affects the vibrational mode of the Y_Z tyrosine, and occupations of the Ca^{2+} site by cations with ionic radii larger than that of Ca^{2+} induce additional distortion in the protein structure in the vicinity of the Mn cluster, including the loss of the vibrational mode of the histidine ligand of the Mn cluster. We propose that the function of the Ca^{2+} ion in OEC is toward the formation of the hydrogen bond network for the proton-coupled electron transfer, which is essential to the water oxidation.

REFERENCES

1. Tommos, C., and Babcock, G. T. (2000) *Biochim. Biophys. Acta 1458*, 199−219.
2. Robblee, J. H., Cinco, R. M., and Yachandra, V. K. (2001) *Biochim. Biophys. Acta 1503*, 7−23.
3. Renger, G. (2001) *Biochim. Biophys. Acta 1503*, 210−228.
4. Vrettos, J. S., Limburg, J., and Brudvig, G. W. (2001) *Biochim. Biophys. Acta 1503*, 229−245.
5. Ghanotakis, D. F., Babcock, G. T., and Yocum, C. F. (1984) *FEBS Lett. 167*, 127−130.
6. Ono, T.-A., and Inoue, Y. (1988) *FEBS Lett. 227*, 147−152.
7. Boussac, A., and Rutherford, A. W. (1988) *Biochemistry 27*, 3476−3483.
8. Boussac, A., and Rutherford, A. W. (1988) *Chem. Scr. 28A*, 123−126.
9. Yocum, C. F. (1991) *Biochim. Biophys. Acta 1059*, 1−15.
10. Debus, R. J. (1992) *Biochim. Biophys. Acta 1102*, 269−352.
11. Ono, T.-A., and Inoue, Y. (1989) *Arch. Biochem. Biophys. 275*, 440−448.
12. Boussac, A., Zimmermann, J.-L., and Rutherford, A. W. (1989) *Biochemistry 28*, 8984−8989.
13. Ono, T.-A., and Inoue, Y. (1990) *Biochim. Biophys. Acta 1020*, 269−277.
14. Boussac, A., Zimmermann, J.-L., Rutherford, A. W., and Lavergne, J. (1990) *Nature 347*, 303−306.
15. Hallahan, B. J., Nugent, J. H. A., Warden, J. T., and Evans, M. C. W. (1992) *Biochemistry 31*, 4562−4573.
16. Latimer, M. J., DeRose, V. J., Mukerji, I., Yachandra, V. K., Sauer, K., and Klein, M. P. (1995) *Biochemistry 34*, 10898−10909.
17. Cinco, R. M., Robblee, J. H., Rompel, A., Fernandez, C., Yachandra, V. K., Sauer, K., and Klein, M. P. (1998) *J. Phys. Chem. B 102*, 8248−8256.
18. Matysik, J., Nachtegaal, G., van Gorkom, H. J., Hoff, A. J., and de Groot, H. J. M. (2000) *Biochemistry 39*, 6751−6755.
19. Riggs-Gelasco, P. J., Mei, R., Ghanotakis, D. F., Yocum, C. F., and Penner-Hahn, J. E. (1996) *J. Am. Chem. Soc. 118*, 2400−2410.
20. Booth, P. J., Rutherford, A. W., and Boussac, A. (1996) *Biochim. Biophys. Acta 1277*, 127−134.
21. Chu, H.-A., Nguyen, A. P., and Debus, R. J. (1995) *Biochemistry 34*, 5839−5858.
22. Debus, R. J. (2001) *Biochim. Biophys. Acta 1503*, 164−186.
23. Zouni, A., Witt, H.-T., Kern, J., Fromme, P., Krauss, N., Saenger, W., and Orth, P. (2001) *Nature 409*, 739−743.
24. Ghanotakis, D. F., Babcock, G. T., and Yocum, C. F. (1985) *Biochim. Biophys. Acta 809*, 173−180.
25. Waggoner, C. M., Pecoraro, V., and Yocum, C. F. (1989) *FEBS Lett. 244*, 237−240.
26. Waggoner, C. M., and Yocum, C. F. (1990) in *Current Research in Photosynthesis* (Baltscheffsky, M., Ed.) Vol. I, pp 733−736, Kluwer, Dordrecht.
27. Bakou, A., Buser, C., Dandulakis, G., Brudvig, G., and Ghanotakis, D. F. (1992) *Biochim. Biophys. Acta 1099*, 131−136.
28. Ono, T.-A. (2000) *J. Inorg. Biochem. 82*, 85−91.

29. Ono, T.-A., Rompel, A., Mino, H., and Chiba, N. (2001) *Biophys. J. 81*, 1831−1840.
30. Vrettos, J. S., Stone, D. A., and Brudvig, G. W. (2001) *Biochemistry 40*, 7937−7945.
31. Martin, R. B. (1984) *Met. Ions Biol. Syst. 17*, 1−49.
32. Noguchi, T., Ono, T.-A., and Inoue, Y. (1992) *Biochemistry 31*, 5953−5956.
33. Noguchi, T., Ono, T.-A., and Inoue, Y. (1995) *Biochim. Biophys. Acta 1228*, 189−200.
34. Noguchi, T., Ono, T.-A., and Inoue, Y. (1995) *Biochim. Biophys. Acta 1232*, 59−66.
35. Noguchi, T., and Inoue, Y. (1995) *J. Biochem. 118*, 9−12.
36. Hienerwadel, R., and Berthomieu, C. (1995) *Biochemistry 34*, 16288−16297.
37. Noguchi, T., Inoue, Y., and Tang X.-S. (1997) *Biochemistry 36*, 14705−14711.
38. Hienerwadel, R., Boussac, A., Breton, J., Diner, B. A., and Berthomieu, C. (1997) *Biochemistry 36*, 14712−14723.
39. Zhang, H., Razeghifard, M. R., Fischer, G., and Wydrzynski, T. (1997) *Biochemistry 36*, 11762−11768.
40. Zhang, H., Fischer, G., and Wydrzynski, T. (1998) *Biochemistry 37*, 5511−5517.
41. Berthomieu, C., Hienerwadel, R., Boussac, A., Breton, J., and Diner, B. A. (1998) *Biochemistry 37*, 10547−10554.
42. Noguchi, T., Inoue, Y., and Tang, X.-S. (1999) *Biochemistry 38*, 10187−10195.
43. Chu, H.-A., Sackett, H., and Babcock, G. T. (2000) *Biochemistry 39*, 14371−14376.
44. Noguchi, T., and Sugiura, M. (2000) *Biochemistry 39*, 10943−10949.
45. Chu, H.-A., Hillier, W., Law, N. A., and Babcock, G. T. (2001) *Biochim. Biophys. Acta 1503*, 69−82.
46. Noguchi, T., and Sugiura, M. (2001) *Biochemistry 40*, 1497−1502.
47. Hillier, W., and Babcock, G. T. (2001) *Biochemistry 40*, 1503−1509.
48. Chu, H.-A., Debus, R. J., and Babcock, G. T. (2001) *Biochemistry 40*, 2312−2316.
49. Berthomieu, C., and Hienerwadel, R. (2001) *Biochemistry 40*, 4044−4052.
50. Kimura, Y., and Ono, T.-A. (2001) *Biochemistry 40*, 14061−14068.
51. Berthold, D. A., Babcock, G. T., and Yocum, C. F. (1981) *FEBS Lett. 134*, 231−234.
52. Ono, T.-A., and Inoue, Y. (1986) *Biochim. Biophys. Acta 850*, 380−389.
53. Silva, J. J. R. F., and Williams, R. J. P. (2001) *The biological chemistry of the elements*, 2nd ed., pp 39−51, Oxford University Press, Oxford.
54. Turconi, S., Horwitz, C. P., Ciringh, Y., Weintraub, S. T., Warden, J. T., Nugent, J. H. A., and Evans, M. C. W (1997) *J. Chem. Soc., Dalton Trans. 2*, 4075−4082.
55. Gilchrist, M. L., Jr., Ball, J. A., Randall, D. W., and Britt, R. D. (1995) *Proc. Natl. Acad. Sci. U.S.A. 92*, 9545−9549
56. Hoganson, C. W., Lydakis-Simantiris, N., Tang, X.-S., Tommos, C., Warncke, K., Babcock, G. T., Diner, B. A., MaCracken, J., and Styring, S. (1995) *Photosynth. Res. 46*, 177−184.
57. Hoganson, C. W., and Babcock, G. T. (1997) *Science 277*, 1953−1956.
58. Hallahan, B. J., Nugent, J. H. A, Warden, J. T., and Evans, M. C. W. (1992) *Biochemistry 31*, 4562−4573.
59. Tang, X.-S., Randall, D. W., Force, D. A., Diner, B. A., and Britt, R. D. (1996) *J. Am. Chem. Soc. 118*, 7638−7639.
60. Peloquin, J. M., Campbell, K. A., and Britt, R. D. (1998) *J. Am. Chem. Soc. 120*, 6840−6841.
61. Astashkin, A. V., Mino, H., Kawamori, A., and Ono, T.-A. (1997) *Chem. Phys. Lett. 272*, 506−516.
62. Mino, H., Kawamori, A., and Ono, T.-A. (2000) *Biochemistry 39*, 11034−11040.
63. Geijer, P., Morvaridi, F., and Styring, S. (2001) *Biochemistry 40*, 10881−10891.
64. Baumgarten, M., Philo, J. S., and Dismukes, G. C. (1990) *Biochemistry 29*, 10814−10822.
65. Boussac, A., Sétif, P., and Rutherford, A. W. (1992) *Biochemistry 31*, 1224−1234.
66. Klimov, V. V., and Baranov, S. V. (2001) *Biochim. Biophys. Acta 1503*, 187−196.
67. Dismukes, G. C., Klimov, V. V., Baranov, S. V., Kozlov, Yu. N., DasGupta, J., and Tyryshkin, A. (2001) *Proc. Natl. Acad. Sci. U.S.A. 98*, 2170−2175.

BI016093U